ACS OMEGA

http://pubs.acs.org/journal/acsodf

Article

Trapping Hydrogen Atoms in Vacancies of Li_2TiO_3 Crystal: A First-Principles Study

Jin-Yang Su, Yan-Wei Li, Wei-Hua Wang, Kun Li,* and Wen Yang*

Cite This: *ACS Omega* 2022, 7, 27149−27156

Read Online

ACCESS | Metrics & More | Article Recommendations | Supporting Information

ABSTRACT: The hydrogen atom capacity in the vacancies of the Li_2TiO_3 crystal is systematically studied by the first-principles method to evaluate its tritium release performance as a solid breeder material in nuclear fusion reactors. The adsorption process of adding hydrogen atoms one by one in the vacancy are investigated to find the possible adsorption sites of the hydrogen atoms in the vacancy. The charge transfer and density of states analysis are performed to reveal the form of a hydrogen−hydrogen dimer in the vacancy. Also, the trapping energy and formation energy are defined and calculated to determine the hydrogen atom capacity of the system. According to the simulations, the Ti vacancies have the strongest hydrogen atom capacity followed by Li vacancies, and O vacancies are the weakest. The influence of hydrostatic pressure on the hydrogen atom capacity is also investigated. Our results reveal the hydrogen capacity of vacancies in the Li_2TiO_3 crystal from the atomic scale, which also provide a theoretical guide to the related tritium release experiments.

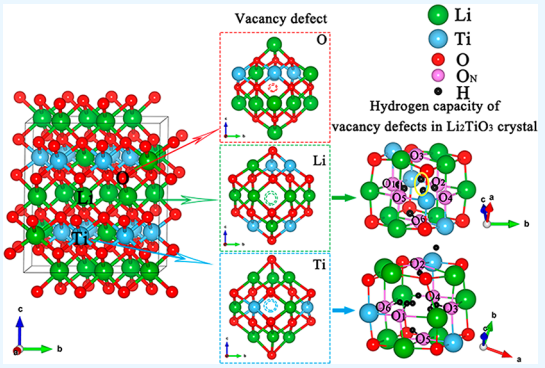

1. INTRODUCTION

Tritium is an isotope of hydrogen. At present, the deuterium−tritium fusion reaction has been widely focused to solve energy problems. As a nuclear fuel, deuterium can be extracted in large quantities from seawater. However, due to the short half-life of tritium, it cannot be obtained directly in nature.[1] Now, tritium is generally extracted by the transmutation reaction in lithium-containing ceramic breeder materials. Among varieties of potential breeder materials,[2−6] Li_2TiO_3 has been widely studied due to its good chemical stability and tritium release behavior.[7−9]

Most current experiments are working on the preparation and its effect on the tritium release performance. Tan et al. employed a non-hydrolytic sol−gel method to obtain Li_2TiO_3 ceramic particles with a grain size of 2.85 μm and porosity of 19.84%,[10] which is beneficial to the tritium release process. Guo et al. implemented the rolling method sintered in air and vacuum[11] and found that ceramic pebbles sintered in air have lower porosity and higher Li content than those sintered in vacuum, which resulted in a higher tritium release rate of the pebbles. Wang et al. used 2 MeV He ions and 10 MeV O ions to irradiate the Li_2TiO_3 crystal and obtained Ti^{3+} defects under O ion irradiation.[12] Kobayashi et al. established a tritium release model with radiation-induced defects,[13] which increased the tritium storage capacity but reduced the tritium release capacity of Li_2TiO_3 materials. In addition, Li_2TiO_3 crystals can be prepared by changing external conditions.[14] It was also found that irradiation and high temperature could reduce the tritium recovery.[15] Various methods have been used to improve the tritium release performance of Li_2TiO_3 crystals.

According to the theoretical work, the previous study mainly focused on the internal and surface structure of the Li_2TiO_3 crystal. Azuma et al. determined that the most stable surface of the Li_2TiO_3 crystal is the Li-terminated (001) surface through calculations and STM observations.[16,17] Moreover, the 1/3 Li-terminated (001) surface obtained by Jiang et al. through first-principles calculations was consistent with the observations of STM.[18] Fang et al. found by DFT calculations that the Si-doped Li_2TiO_3 surface promoted the formation of T_2O (Tritium oxide).[19] In addition, there are theoretical research studies on Li defects,[20] the diffusion of Li atom[21] and tritium atom[22,23] in the Li_2TiO_3 crystal. However, there is no systematic demonstration of the tritium trapping capacity in the vacancies generated in the Li_2TiO_3 crystal so far, either experimentally or theoretically. Therefore, here, we use first-principles calculations to analyze the generation of vacancies in the Li_2TiO_3 crystal and its tritium trapping capacity is calculated accordingly. The H and T atoms are identical in chemical properties but different in kinetic properties. Since

Received: March 14, 2022
Accepted: July 14, 2022
Published: July 25, 2022

the kinetic properties are not involved in this work, the isotopic effects can be ignored here. For the density functional theory (DFT) simulations, the tritium (T) atom is usually treated as a hydrogen atom[12,19] as they presented same electronic properties. Therefore, the hydrogen trapping capacity is equivalent to the tritium trapping capacity in this work.

In this work, we conduct a comprehensive first-principles study of the hydrogen atom capacity in the Li_2TiO_3 crystal. Defect models with eight types of vacancies including Li vacancy, Ti vacancy, and O vacancy are built up and optimized first. Then, the hydrogen atom is added in the vacancy one by one and fully relaxed to determine the adsorption sites of the hydrogen atom in each type of vacancies. The trapping energy and formation energy are defined and calculated to analyze the hydrogen atom capacity from two aspects. The influence of hydrostatic pressure on the hydrogen atom capacity is investigated as well. The obtained results are also compared with related experiments and explain the mechanism of the hydrogen atom capacity of vacancies in the Li_2TiO_3 crystal.

2. THEORETICAL MODEL AND METHODS

In this study, three types of defect models of the Li_2TiO_3 crystal with vacancies were built up and calculated by the Vienna ab initio simulation package (VASP).[24,25] The generalized gradient approximation (GGA)[26] of Perdew–Burke–Ernzerhof (PBE)[27] and the projector-augmented wave method (PAW)[28] were implemented in the simulations. After benchmark calculations, the plane wave cutoff energy was determined as 600 eV and the K-point was set as $4 \times 4 \times 4$ for geometry optimization and $2 \times 1 \times 2$ for other calculations. The total energy was converged to 10^{-5} eV, and all the structures were fully relaxed when the maximum force on each atom was less than 0.003 eV/Å.

In order to analyze the generation of vacancies in the crystal, the formation energy of vacancy $E_v(x)$ is defined as:

$$E_v(x) = E(Li_2TiO_3{:}\ V_x) - E(Li_2TiO_3) + E(x) \quad (1)$$

Where $E(Li_2TiO_3{:}V_x)$ is the total energy of a defect supercell with a vacancy of x atom (V_x), $E(Li_2TiO_3)$ is the total energy of the corresponding perfect supercell, and $E(x)$ is the chemical potential of the x atom. The chemical potential of the Li atom is used as −1.825 eV, that of Ti is −6.943 eV, and that of the O atom is −4.233 eV.

For the analysis of hydrogen capacity in the vacancy, there has not been a standard energy definition by now. Here, we define two types of energies including trapping energy E_{trap} and formation energy E_f to determine the hydrogen capacity of atomic vacancies in Li_2TiO_3 crystals, from two different aspects. The following E_{trap} represents the energy required for a hydrogen atom to move from an interstitial adsorption site outside the vacancy to an adsorption site inside the vacancy.

$$E_{trap} = E(V_x, mH) - E[V_x, (m-1)H] - [E(V_x, H) - E(Li_2TiO_3{:}\ V_x)] \quad (2)$$

where $E(V_x,mH)$ or $E[V_x,(m-1)H]$ is total energy of the system with m or $m-1$ hydrogen atoms adsorbed inside the vacancy of V_x, $E(V_x,H)$ is the total energy of system with a V_x vacancy and a hydrogen atom adsorbed in an interstitial site outside the vacancy. $E(V_x, mH) - E[V_x, (m-1)H] - \frac{1}{2}E(H_2)$ is the adsorption energy of the m_{th} H atom adsorbed inside the vacancy, while $E(V_x, H) - E(Li_2TiO_3{:}\ V_x) - \frac{1}{2}E(H_2)$ represents the adsorption energy of a H atom adsorbed in an interstitial site outside the vacancy. When the two energies are subtracted, we get eq 2, namely, E_{trap}, which represents the H adsorption energy from the interstitial site outside the vacancy to the adsorption site inside the vacancy.

Moreover, the formation energy E_f is defined according to the traditional definition of the formation energy as:

$$E_f = E(V_x, mH) - m\frac{1}{2}E(H_2) - E(Li_2TiO_3{:}\ V_x) \quad (3)$$

where $E(H_2)$ is the total energy of a H_2 molecule. In the calculation of formation energy E_f, the energy of a hydrogen atom is half of the energy of H_2, and it is the hydrogen atom energy diffused in the crystal in the calculation of the trapping energy E_{trap}. Therefore, the E_{trap} corresponds to the H adsorption energy from an interstitial adsorption site outside the vacancy to an adsorption site inside the vacancy, which denotes the lowest hydrogen capacity. The E_f corresponds to the H adsorption energy from the free state (H_2, outside the crystal) to an adsorption site inside the vacancy, which represents the highest hydrogen capacity in the vacancy of V_x. The trapping energy E_{trap} and formation energy E_f provide a range of hydrogen capacity, which comprehensively analyze the hydrogen atom capacity in Li_2TiO_3 crystals.

3. RESULTS AND DISCUSSION

3.1. Structure of Perfect and Defect Model of Li_2TiO_3 Crystal. According to the related experimental work,[29] the perfect model of a $2 \times 2 \times 1$ supercell ($Li_{64}Ti_{32}O_{96}$) with C2/c symmetry is built upon a unit cell of $Li_{16}Ti_8O_{24}$, which is plotted in Figure 1. The perfect crystal is stacked by three types of layers, pure-Li layer, pure-O layer, and Li–Ti layer. The structure of perfect crystal is fully relaxed, and the lattice parameters are obtained as a = 5.0936 Å, b = 8.8420 Å, c = 9.8136 Å, and β = 100.214°, which are close to the experimental results of a = 5.0623 Å, b = 8.7876 Å, c = 9.7533 Å, and β = 100.212°.[29]

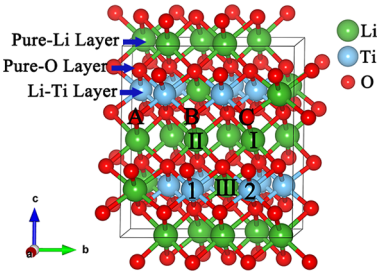

Figure 1. Unit cell structure of the Li_2TiO_3 crystal.

As shown in Figure 1, there are three types of Li atoms (I/II/III), two types of Ti atoms (1/2), and three types of O atoms (A/B/C) which are labeled in Figure 1. The defect models of the Li_2TiO_3 crystal in presence with vacancy are set up accordingly by removing one atom in the perfect model. Defect models with three types of Li vacancies are optimized and presented in Figure 2. When a Li atom is missing, six neighboring oxygen atoms, which were bonded with this Li atom, will form dangling bonds instead. As shown in the cage configurations of each type of Li vacancy ($V_{Li\text{-}I}$, $V_{Li\text{-}II}$, $V_{Li\text{-}III}$) in Figure 2, the oxygen atoms with dangling bonds are plotted as

https://doi.org/10.1021/acsomega.2c01532
ACS Omega 2022, 7, 27149−27156

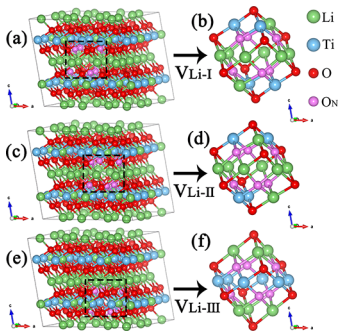

Figure 2. Defect models of the Li_2TiO_3 crystal with Li vacancy. (a, c, e): Relative positions of Li-I vacancy (V_{Li-I}), Li-II vacancy (V_{Li-II}), and Li-III vacancy (V_{Li-III}) in the crystal; (b, d, f) sketch map of the cage configuration of each type of Li vacancy.

pink balls (O_N) to distinguish with other saturated red oxygen atoms (O). Li-I/Li-II atoms are in the pure-Li layer in the Li_2TiO_3 crystal, and Li-III atoms are in the Li−Ti layer of the crystal. The relative positions of each type of vacancy are presented in Figure 2a,c,e. The cage formed by Li-I/Li-II atomic vacancy defects contains 14 O atoms, 4 Ti atoms, and 8 Li atoms as shown in Figure 2b,d. The cage formed by Li-III atomic vacancy defects contains 14 O atoms, 6 Li atoms, and 6 Ti atoms as shown in Figure 2f.

Figure 3a,c presents the relative positions of the defect models with two types of Ti vacancies (V_{Ti-1}, V_{Ti-2}). Also, the

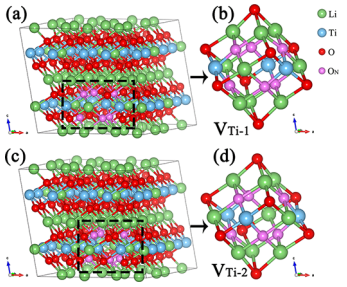

Figure 3. Defect models of the Li_2TiO_3 crystal with Ti vacancy. (a, c) Relative positions of Ti-1 vacancy (V_{Ti-1}) and Ti-2 vacancy (V_{Ti-2}) in the crystal; (b, d) sketch map of the cage configuration of each Ti vacancy.

corresponding cage configurations in Figure 3b,d show that there are also six oxygen atoms with dangling bonds (O_N) in each vacancy. Moreover, there are totally 14 O atoms, 9 Li atoms, and 3 Ti atoms in the cage configurations of both Ti-1 and Ti-2 vacancy defects. Three types of defect models with O vacancies are illustrated in Figure 4. When an O atom is missing, the neighboring two Ti atoms and four Li atoms will form dangling bonds. In Figure 4, the green balls represent saturated Li atoms (Li), while the gray balls represent Li atoms with dangling bonds (Li_N). The blue balls are saturated Ti atoms (Ti), and the purple balls are Ti atoms with dangling bonds (Ti_N). There are 12 O atoms, 9 Li atoms, and 5 Ti atoms in each type of the O vacancy defect (O-A/O-B/O-C) in the Li_2TiO_3 crystal as shown in Figure 4b,d,f.

All the other representations in Figures 2−4 are identical to Figure 1. In addition, the formation energy of each defect model has been calculated by eq 1 and presented in Table 1. It is found that the formation energy of defect model with Li vacancy is the lowest, and the formation energy with Ti

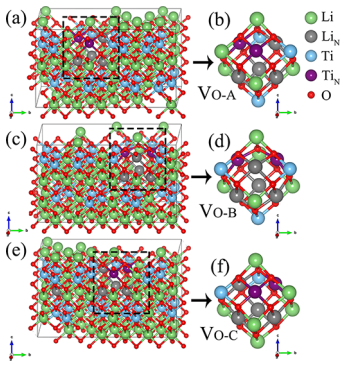

Figure 4. Defect models of Li_2TiO_3 crystal with O vacancy. (a, c, e): Relative positions of O-A vacancy (V_{O-A}), O-B vacancy (V_{O-B}), and O-C vacancy (V_{O-C}) in the crystal; (b, d, f): sketch map of the cage configuration of each type of O vacancy.

Table 1. Formation Energy $E_v(x)$ of each Defect Model

	E_v(Li) (eV)		E_v(Ti) (eV)		E_v(O) (eV)
V_{Li-I}	4.788	V_{Ti-1}	15.261	V_{O-A}	6.063
V_{Li-II}	4.785	V_{Ti-2}	15.256	V_{O-B}	6.145
V_{Li-III}	4.679			V_{O-C}	6.233

vacancy is the highest. Also, the formation energy of Li vacancy is consistent with the previous work.[21]

3.2. Hydrogen Atom Capacity in the Li Vacancy of Li_2TiO_3 Crystal. In the Li_2TiO_3 crystal containing Li vacancy, the missing Li atom changes the stability of the six neighboring O atoms. In Figure 5a, the pink balls labeled with number of 1−6 represent six neighboring O atoms (O1−O6) of the missing Li atom. These neighboring O atoms with dangling bonds constitute an octahedral cage configuration. We place the hydrogen atoms one by one in such an octahedral cage of the crystal in order to obtain the hydrogen capacity of the vacancy. The adsorption sites of 1−6 hydrogen atoms in the Li-I vacancy are calculated and presented in Figure 5b−g. Meanwhile, in the process of accommodating H atoms in the Li-I vacancy, the evolution of the vacancy structure is described by measuring the distances of O1−O4, O2−O5, and O3−O6 and the corresponding results are presented in Table 2. It is clear that the cage formed by Li vacancy defect mainly increases when more H atoms are adsorbed in the vacancy.

In our simulations, we have studied the different adsorption sites of H in the vacancy as much as possible to determine the stable H adsorption site. Considering the three-dimensional coordinate system of the cage structure of the vacancy, the initial position of the first hydrogen atom is on the line between the cage center and an O atom with dangling bond, 0.7 Å from the cage center and 1.5 Å from the O atom. As there are totally six O atoms (O1−O6) in the cage, there are six initial positions of the hydrogen atom. The hydrogen atom is placed in six initial positions, and the total defect model is fully relaxed. After relaxations, the H atom deviates from the initial position and arrives at corresponding six adsorption sites. Then, the adsorption energies are calculated and compared for the six adsorption sites. The results show that the adsorption energy is the lowest when the hydrogen atom is adsorbed at the O atom of O4 and the H−O4 bond length is 0.984 Å, as shown in Figure 5b. Thus, site (O4) with the lowest adsorption energy is determined as the stable adsorption site for the first H atom. It is noted that all the

https://doi.org/10.1021/acsomega.2c01532
ACS Omega 2022, 7, 27149−27156

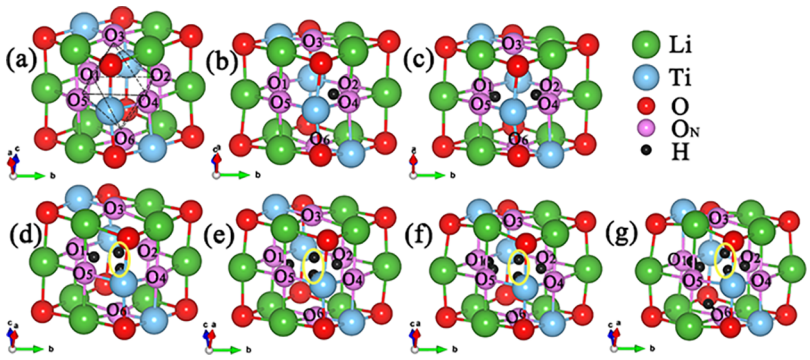

Figure 5. (a) Partial structure of the Li-I vacancy; (b−g) adsorption sites of 1−6 hydrogen atoms (black balls) in the Li-I vacancy.

Table 2. Distances of O1−O4, O2−O5, and O3−O6 in the Li-I Vacancy with Different Numbers of Adsorbed H Atoms

	0-H (Å)	1-H (Å)	2-H (Å)	3-H (Å)	4-H (Å)	5-H (Å)	6-H (Å)
O1−O4	4.104	4.031	3.969	4.413	4.452	4.480	4.468
O2−O5	4.392	4.526	4.495	4.587	4.508	4.486	4.444
O3−O6	4.380	4.499	4.478	4.538	4.507	4.486	4.482

six H atoms tend to move toward the position with the lowest adsorption energy in the cage structure of vacancy, and thus the stable adsorption site (O4) in the vacancy has little correlation with the initial positions we placed. Such an optimized configuration with H adsorbed at O4 is used as the initial configuration for placing the second hydrogen atom.

Based on the configuration with the first hydrogen atom in Figure 5b, we place the second hydrogen atom on the remaining five adsorption sites except O4 and relax the system in the same way. The result shows that the stable adsorption site of the second hydrogen atom is on the O1 site and the H−O1 bond length is 0.981 Å, as shown in Figure 5c. It is noted that the adsorption of the second hydrogen atom has little influence of the first hydrogen atom, and thus the first hydrogen atom is still adsorbed on the O4 site. Then, the optimized system configuration is used as the initial configuration for placing the third hydrogen atom. When the third hydrogen atom is added in the vacancy and optimized in the same way, it is interesting to find that the third hydrogen atom does not bond with the nearest O3 atom but bonds with the first hydrogen atom instead to form a hydrogen dimer in the vacancy. Meanwhile, the H−O4 bond of the first hydrogen atom has been broken due to the addition of the third hydrogen atom. The formed hydrogen dimer locates close to the center of the octahedral cage, which is circled in Figure 5d. When the fourth hydrogen atom is placed in the vacancy in Figure 5e, it bonds with the O2 atom. When the fifth and sixth hydrogen atoms are added in the vacancy, the adsorption sites are O5 and O6 but with large lattice distortion and high adsorption energy. At the same time, the formed hydrogen dimer is close to the center of the vacancy in Figure 5e−g.

The charge transfer of the neighboring oxygen atoms (O1−O6) is counted in Table 3 to further demonstrate the formation of the H−H dimer in the Li vacancy. In Table 3, all six O atoms with dangling bands (O1−O6) have a similar charge of about 7.1 eV. When the first H atom enters the vacancy, the Bader charge of the O4 atom increases from 7.140

Table 3. Bader Charge of the Oxygen Atoms (O1−O6) in the Octahedral Cage of Li-I Vacancy with 1−6 Adsorbed Hydrogen Atoms, Respectively

atom	V_{Li-I}	1-H	2-H	3-H	4-H	5-H	6-H
O1	7.140	7.157	7.317	7.309	7.304	7.325	7.297
O2	7.130	7.150	7.161	7.131	7.291	7.309	7.303
O3	7.126	7.148	7.158	7.140	7.151	7.167	7.164
O4	7.140	7.316	7.320	7.148	7.168	7.168	7.171
O5	7.130	7.147	7.162	7.132	7.136	7.254	7.273
O6	7.126	7.142	7.158	7.144	7.156	7.162	7.240

to 7.316 eV while the charge of other O atoms changing only about 0.02 eV. This indicates the formation of the H−O4 bond. When the second H atom is adsorbed in the vacancy, the charge of the O1 atom obviously increases and that of the other O atoms changes a little bit.

When the third H atom is placed in the vacancy, the charge of all the O atoms decrease. And the decrease of O4 atom is the most dramatic one which charge changes from 7.320 to 7.148 eV in Table 3. This fact proves the H−O4 bond breaking when the third H atom is added in the vacancy. At the same time, the density of states of the three H atoms are also plotted in Figure 6, which further demonstrates the formation of the H−H dimer with the third H and the first H atoms. When the fourth, fifth, and sixth H atoms enters the Li vacancy, the charges of the O2, O5, and O6 atoms increase, which proves that the corresponding H−O bonds formed in

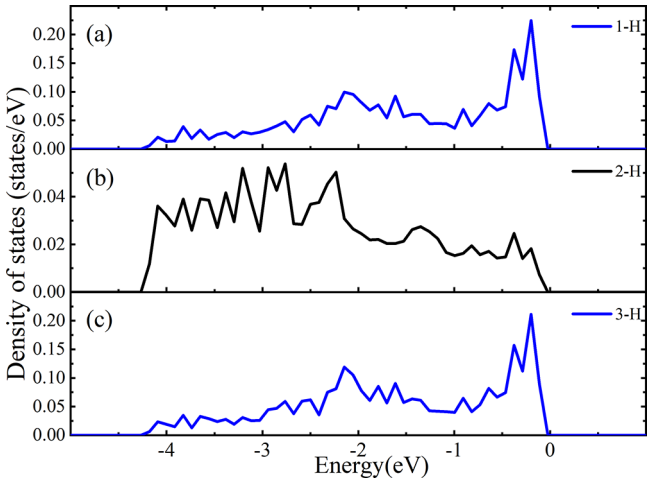

Figure 6. Density of states of three hydrogen atoms of (a) 1-H, (b) 2-H, and (c) 3-H adsorbed in the Li-I vacancy.

https://doi.org/10.1021/acsomega.2c01532
ACS Omega 2022, 7, 27149−27156

Table 4. Trapping Energy E_{trap} and Formation Energy E_f for Systems with 1−6 Adsorbed Hydrogen Atoms in Three Types of Li Vacancies

number of H atoms	E_{trap} (Li-I) (eV)	E_{trap} (Li-II) (eV)	E_{trap} (Li-III) (eV)	E_f (Li-I) (eV)	E_f (Li-II) (eV)	E_f (Li-III) (eV)
1	−0.683	−0.846	−0.755	−2.449	−2.471	−2.369
2	2.361	2.346	2.319	−1.853	−1.750	−1.664
3	2.514	2.212	2.542	−1.105	−1.163	−0.736
4	2.674	2.420	2.276	−0.196	−0.368	−0.074
5	2.853	2.689	2.739	0.892	0.696	1.051
6	3.004	2.851	2.635	2.131	1.921	2.072

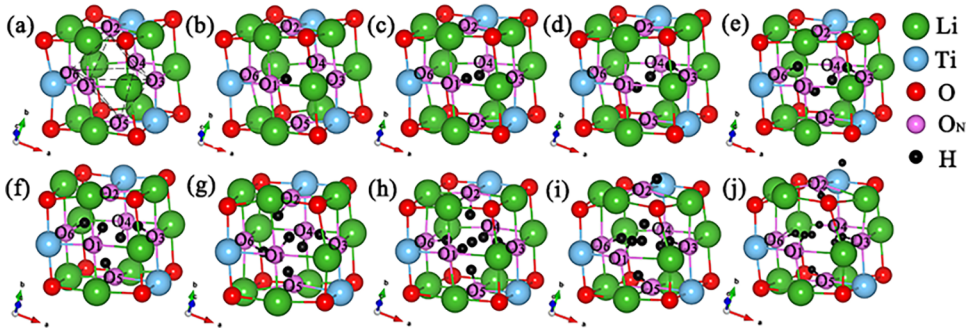

Figure 7. (a) Partial structure of the Ti-1 vacancy; (b−j) adsorption sites of 1−9 hydrogen atoms (black balls) in the Ti-1 vacancy, respectively.

Table 5. Distances of O1−O4, O2−O5, and O3-O6 in the Ti-1 Vacancy with Different Numbers of Adsorbed H Atoms

	0-H (Å)	1-H (Å)	2-H (Å)	3-H (Å)	4-H (Å)	5-H (Å)	6-H (Å)	7-H (Å)	8-H (Å)	9-H (Å)
O1−O4	4.285	4.140	4.070	4.115	4.173	4.149	4.218	4.529	4.467	4.440
O2−O5	4.285	4.251	4.267	4.137	3.976	3.862	3.824	4.530	4.562	4.634
O3−O6	4.333	4.336	4.285	4.287	4.229	4.280	4.299	4.513	4.506	4.516

the vacancy. All these results are consistent with those of the above adsorption sites of the six H atoms in the Li-I vacancy.

At the same time, the trapping energy E_{trap} and formation energy E_f have been calculated to analyze the hydrogen atom capacity on the basis of the above adsorption process of hydrogen atoms in the Li vacancy. E_{trap} and E_f of systems with 1−6 adsorbed hydrogen atoms in each type of Li vacancy are presented in Table 4. As defined above, the trapping energy E_{trap} denotes the lowest hydrogen capacity, while the E_f represents the highest hydrogen capacity in the vacancy. It is found that the trapping energy E_{trap} increases with the increasing number of hydrogen atoms. Also, we can see that E_{trap} is negative only when one hydrogen atom is adsorbed in the Li vacancy. This fact proves that the Li vacancy can at least spontaneously accommodate one hydrogen atom. For the formation energy E_f, it changes from negative to positive when the fifth H atom is added in the Li vacancy, which indicates that the vacancy can spontaneously accommodate four hydrogen atoms at most.

It is noted that the hydrogen capacity of three types of Li vacancies is the same, although the values of E_{trap} and E_f are different, but the change trend is the same. In addition, although the fifth H and sixth H atoms can be adsorbed in the Li vacancy in Figure 5f−g, this results in large lattice distortion and high adsorption energy. In combination with the results of E_{trap} and E_f, it is obtained that the Li vacancy cannot spontaneously adsorb the fifth and the sixth H atoms. Therefore, we conclude that each type of Li vacancy can spontaneously accommodate 1−4 hydrogen atoms in the Li_2TiO_3 crystal.

3.3. Hydrogen Atom Capacity in the Ti Vacancy of Li_2TiO_3 Crystal. In this section, the adsorption sites of hydrogen atoms in the Ti vacancy are found and the hydrogen atom capacity is systematically analyzed. The methods used are the same to those used for the Li vacancy. In Figure 7a, the six neighboring O atoms (O1−O6) with dangling bonds in the Ti vacancy also constitute an octahedral cage, which is similar to that in the Li vacancy. Then, we place the hydrogen atoms one by one in the octahedral cage and obtain the corresponding adsorption sites of 1−9 hydrogen atoms in the Ti-1 vacancy, as shown in Figure 7b−j. The adsorption sites are found by the calculations of adsorption energy. During the process of accommodating H atoms in the Ti-1 vacancy, the distances of O1−O4, O2−O5, and O3−O6 are also measured and presented in Table 5. The distortion of the Ti vacancy defect also increases with the increasing number of adsorbed H atoms.

In Figure 7b−g, when 1−6 hydrogen atoms are placed successively in the Ti vacancy, the hydrogen atoms are adsorbed at O1, O4, O3, O6, O5, and O2, respectively. In other words, the hydrogen atoms bond with the corresponding neighboring O atoms in the Ti vacancy. The corresponding Bader charge of the neighboring O atoms (O1−O6) in Table 6 also proves these results. Figure 7h shows that the added seventh hydrogen atom is not adsorbed by any atoms but is located close the center of the Ti vacancy. When adding the eighth hydrogen atom into the vacancy, it is found that the eighth hydrogen atom forms a H−H bond with the seventh hydrogen atom located in the center of the vacancy. At the same time, the internal space of the vacancy is getting smaller with the increasing number of atoms in the vacancy, which

https://doi.org/10.1021/acsomega.2c01532
ACS Omega 2022, 7, 27149−27156

Table 6. Bader Charge of the Oxygen Atoms (O1−O6) in the Octahedral Cage of Ti-1 Vacancy with 1−6 Adsorbed Hydrogen Atoms, Respectively

atom	V_{Ti-1}	1-H	2-H	3-H	4-H	5-H	6-H
O1	7.070	7.323	7.317	7.314	7.325	7.344	7.288
O2	7.064	7.091	7.134	7.160	7.180	7.192	7.314
O3	7.089	7.134	7.164	7.378	7.318	7.361	7.331
O4	7.064	7.079	7.338	7.339	7.315	7.333	7.292
O5	7.070	7.098	7.147	7.178	7.188	7.289	7.334
O6	7.089	7.129	7.145	7.164	7.317	7.335	7.351

causes the H−O2 bond be squeezed out of the vacancy. When the ninth hydrogen atom is placed in the vacancy, the H−O2 bond is broken and a hydrogen atom is squeezed out of the vacancy and dissociated into the crystal. At the same time, a new H−O2 bond is formed in the vacancy.

The trapping energy E_{trap} and formation energy E_f are calculated as well to analyze the hydrogen atom capacity in combination with the adsorption process of hydrogen atoms in the Ti vacancy. E_{trap} and E_f for systems with 1−9 adsorbed hydrogen atoms in each type of Ti vacancy are presented in Table 7. For the trapping energy, the negative E_{trap} turns to be

Table 7. Trapping Energy E_{trap} and Formation Energy E_f for Systems with 1−9 Hydrogen Atoms in Two Types of Ti Vacancies

number of H atoms	E_{trap}(Ti-1) (eV)	E_{trap}(Ti-2) (eV)	E_f(Ti-1) (eV)	E_f(Ti-2) (eV)
1	−1.108	−1.123	−2.835	−2.830
2	−0.952	−1.003	−5.514	−5.540
3	−0.654	−0.656	−7.896	−7.903
4	−0.600	−0.605	−10.223	−10.215
5	2.489	2.499	−9.461	−9.423
6	2.814	2.604	−8.374	−8.526
7	2.355	2.495	−7.746	−7.738
8	3.133	2.771	−6.340	−6.674
9	2.828	3.385	−5.239	−4.996

positive when the fifth hydrogen atom is adsorbed in the Ti vacancy. This indicates that the Ti vacancy can at least spontaneously accommodate four hydrogen atoms.

At the same time, the formation energy E_f is negative and decreased until the number of hydrogen atoms increases to five. Namely, the vacancy structure is getting more stable when four or less hydrogen atoms are adsorbed in the vacancy. This further confirms the minimum hydrogen capability obtained from the trapping energy. Also, this is mainly due to the high formation energy of about 15.26 eV of the Ti vacancy in Table 1. For such a Ti vacancy, the adsorption of hydrogen atoms (less than five hydrogen atoms), which compensates for the energy required to form a Ti vacancy, is beneficial to the stability of the structure. Then, when five or more hydrogen atoms are adsorbed, the E_f increases with the number of hydrogen atoms. It is noted that all the formation energies are negative even when nine hydrogen atoms are adsorbed in the Ti vacancy in Table 7. Meanwhile, according to the adsorption structure in Figure 7j, the ninth hydrogen atom actually has been squeezed out of the vacancy. Therefore, we conclude that the Ti vacancy can spontaneously accommodate eight hydrogen atoms at most. The negative formation energies in Table 7, which are calculated by eq 4, may result from the high formation energy of Ti vacancy in Table 1. Generally, we find that each type of Ti vacancy can spontaneously accommodate 4−8 hydrogen atoms in the Li_2TiO_3 crystal.

Moreover, the hydrogen atom capacity in the O vacancy is investigated as well. However, the hydrogen atom is hard to bond with the Li and Ti atoms in the O vacancy, and thus the O vacancy can only accommodate one hydrogen atom according to our simulations (see Figure S1 and Table S1 in the Supporting Information). As the methods are the same to the above cases of Li and Ti vacancies, here, it is not discussed in detail any more.

Generally, the H adsorption capacities of three types of vacancy defects in Li_2TiO_3 crystals have been systematically calculated and analyzed. When H atoms enter Li vacancy and Ti vacancy, they are preferably to be adsorbed by O atoms with dangling bonds in the vacancies to form new covalent bonds. Namely, the Li/Ti vacancy tends to attract the H atoms. When more H atoms enter the Li/Ti vacancy, the H atoms tend to exist in the free states until the vacancy is saturated. When the H atom enters the O vacancy, as the Li and Ti atoms in the vacancy propel the H atom, the O vacancy tends to propel the H atoms. Therefore, the H atom capacity of the vacancy in the Li_2TiO_3 is determined by the interaction between H atom and O atoms with dangling bonds in the different vacancies.

3.4. Effect of Hydrostatic Pressure on the Hydrogen Capacity in the Vacancy of Li_2TiO_3 Crystal. In order to further analyze the hydrogen capacity of vacancy in the Li_2TiO_3 crystal, we study the influence of hydrostatic pressure by changing the strain of the system. The formation energy (E_f) for systems under different strains of 0−4% in the Li-I and Ti-1 vacancy are calculated and presented in Table 8 and Table 9, respectively.

Table 8. Formation Energy E_f for Systems with 1−6 Hydrogen Atoms in Li-I Vacancy under Strain from 0 to 4%

number of H atoms	E_f (eV) (strain 0%)	E_f (eV) (strain 1%)	E_f (eV) (strain 2%)	E_f (eV) (strain 3%)	E_f (eV) (strain 4%)
1	−2.449	−2.432	−2.418	−2.406	−2.393
2	−1.853	−1.830	−1.804	−1.784	−1.765
3	−1.105	−1.104	−0.966	−0.908	−0.846
4	−0.196	−0.119	−0.021	0.052	0.127
5	0.892	0.988	1.113	1.207	1.302
6	2.131	2.259	2.424	2.548	2.674

For both cases of Li vacancy and Ti vacancy, the formation energy E_f increases with the increase of the strain. When there

Table 9. Formation Energy E_f for Systems with 1−9 Hydrogen Atoms in Ti-1 Vacancy under Strain from 0 to 4%

number of H atoms	E_f (eV) (strain 0%)	E_f (eV) (strain 1%)	E_f (eV) (strain 2%)	E_f (eV) (strain 3%)	E_f (eV) (strain 4%)
1	−2.835	−2.834	−2.826	−2.820	−2.813
2	−5.514	−5.504	−5.488	−5.476	−5.462
3	−7.896	−7.870	−7.835	−7.808	−7.779
4	−10.223	−10.139	−10.089	−10.048	−10.006
5	−9.461	−9.348	−9.283	−9.232	−9.178
6	−8.374	−8.283	−8.190	−8.117	−8.042
7	−7.746	−7.605	−7.410	−7.260	−7.106
8	−6.340	−6.010	−5.814	−5.665	−5.513
9	−5.239	−5.328	−4.771	−4.581	−4.684

https://doi.org/10.1021/acsomega.2c01532
ACS Omega 2022, 7, 27149−27156

are four hydrogen atoms adsorbed in the Li vacancy and the strain changes from 2 to 3% in Table 8, E_f will change from −0.021 to 0.052 eV. This indicates that the fourth hydrogen atom cannot be spontaneously adsorbed in the Li vacancy under the case of 3% strain. Namely, it seems that the fourth hydrogen atom could be released from the Li vacancy when 3% strain is applied to the system. Therefore, increasing strain can reduce the hydrogen capacity of vacancy defects and improve the hydrogen release performance of the Li_2TiO_3 crystal.

4. CONCLUSIONS

In this work, the hydrogen capacity in the vacancies of the Li_2TiO_3 crystal are thoroughly investigated using DFT calculations. The trapping energy E_{trap} and formation energy E_f, are defined to determine the hydrogen capacity of the system. The H−H dimer is found to be formed in both the Li vacancy and Ti vacancy. For each type of Li vacancy, it can spontaneously accommodate 1−4 hydrogen atoms in the Li_2TiO_3 crystal. Also, we find that each type of Ti vacancy can spontaneously accommodate 4−8 hydrogen atoms. The O vacancy can only accommodate one hydrogen atom at the same time. Also, the H atom capacity of the vacancy in the Li_2TiO_3 is determined by the interaction between H atom and O atoms with dangling bonds in the different vacancies. We also study the influence of hydrostatic pressure on the hydrogen capacity. It is found that increasing strain can reduce the hydrogen capacity of vacancy defects, thus providing a way to improve the hydrogen release performance of the Li_2TiO_3 crystal. Our results reveal the hydrogen capacity of vacancies in the Li_2TiO_3 crystal, which provide theoretical supports to the related tritium release experiments. It is noted that this work does not take into account the effect of temperature and vibrational effects and also neglect the influence of charge and diffusion energy barrier. Therefore, the more accurate H-accommodating capacity of the vacancy defects in the Li_2TiO_3 crystal will be an interesting topic in the next step.

■ ASSOCIATED CONTENT

Supporting Information

The Supporting Information is available free of charge at https://pubs.acs.org/doi/10.1021/acsomega.2c01532.

> Trapping energy E_{trap} and formation energy E_f for systems with 1−2 adsorbed hydrogen atoms in three types of O vacancies and the formation energy (E_f) for systems under different strains of 0−4% in the Ti-2, Li-II, and Li-III vacancies (PDF)

■ AUTHOR INFORMATION

Corresponding Authors

Kun Li − *School of Applied Science, Taiyuan University of Science and Technology, Taiyuan, Shanxi 030024, P. R. China*; Email: likun@tyust.edu.cn

Wen Yang − *School of Applied Science, Taiyuan University of Science and Technology, Taiyuan, Shanxi 030024, P. R. China; Shanxi Key Laboratory of Metal Forming Theory and Technology, School of Material Science and Engineering, Taiyuan University of Science and Technology, Taiyuan, Shanxi 030024, P. R. China;* orcid.org/0000-0003-1067-2129; Email: yangwen@tyust.edu.cn

Authors

Jin-Yang Su − *School of Applied Science, Taiyuan University of Science and Technology, Taiyuan, Shanxi 030024, P. R. China; Shanxi Key Laboratory of Metal Forming Theory and Technology, School of Material Science and Engineering, Taiyuan University of Science and Technology, Taiyuan, Shanxi 030024, P. R. China*

Yan-Wei Li − *Shanxi Key Laboratory of Metal Forming Theory and Technology, School of Material Science and Engineering, Taiyuan University of Science and Technology, Taiyuan, Shanxi 030024, P. R. China*

Wei-Hua Wang − *Department of Electronic Science and Engineering, Key Laboratory of Photo-Electronic Thin Film Device and Technology of Tianjin, Nankai University, Tianjin 300350, P. R. China;* orcid.org/0000-0002-2287-7669

Complete contact information is available at: https://pubs.acs.org/10.1021/acsomega.2c01532

Author Contributions

J.-Y.S. did the conceptualization, methodology, data curation, software, investigation, writing of the original draft, and validation. Y.-W.L. did the software, validation, and visualization. W.-H.W. did the project administration and funding acquisition. K.L. did the conceptualization, formal analysis, funding acquisition, writing of the review and editing, funding acquisition, and supervision. W.Y. did the validation, resource gathering, project administration, and funding acquisition.

Notes

The authors declare no competing financial interest.

■ ACKNOWLEDGMENTS

This work was supported by the National Natural Science Foundation of China (nos. 51871158, 11874223), the STIP of Shanxi (no. 2020 L0349), and Doctors' Initial Foundation of TYUST (no. 20192036).

■ REFERENCES

(1) Kim, J.-I.; Park, Y.-H.; Ahn, M.-Y.; Kishimoto, H.; Lee, Y.; Cho, S. Effects of Sintering Conditions on the Microstructure of Li_2TiO_3 Tritium Breeding Materials. *Fusion Eng. Des.* **2020**, *156*, 111727.

(2) Yuan, Z.; Kong, X.; Ma, S.; Gao, T.; Xiao, C.; Chen, X.; Lu, T. Adsorption and Diffusion Mechanism of Hydrogen Atom on the Li_2O (111) and (110) Surfaces from First Principles Calculations. *J. Nucl. Mater.* **2019**, *513*, 232−240.

(3) Gierszewski, P. Review of Properties of Lithium Metatitanate. *Fusion Eng. Des.* **1998**, *39-40*, 739−743.

(4) Xiang, X.; Zhu, W.; Lu, T.; Gao, T.; Shi, Y.; Yang, M.; Gong, Y.; Yu, X.; Feng, L.; Wei, Y.; Lu, Z. Density Functional Theory Calculations of Point Defects and Hydrogen Isotopes in Li_4SiO_4. *AIP Adv.* **2015**, *5*, 107136.

(5) Paudel, H. P.; Duan, Y. A First-Principles Density Function Theory Study of Tritium Diffusion in Li_2ZrO_3: Application for Producing Tritium. *J. Phys. Chem. C* **2018**, *122*, 28447−28459.

(6) Zhu, D.; Peng, S.; Chen, X.; Gao, X.; Yang, T. Fabrication and Characterization of Li_3TaO_4 Ceramic Pebbles by Wet Process. *J. Nucl. Mater.* **2010**, *396*, 245−250.

(7) Zhang, W.; Zhou, Q.; Xue, L.; Yan, Y. Fabrication of Li_2TiO_3 Pebbles with Small Grain Size Via Hydrothermal and Improved Dry-Rolling Methods. *J. Nucl. Mater.* **2015**, *464*, 389−393.

(8) Qi, Q.; Wang, J.; Xiang, M.; Zhang, Y.; Gu, S.; Luo, G.-N. Mechanism of Vacuum-Annealing Defects and Its Effect on Release Behavior of Hydrogen Isotopes in Li_2TiO_3. *Int. J. Hydrogen Energy* **2018**, *43*, 12295−12301.

(9) Guo, H.; Wang, H.; Chen, R.; Gong, Y.; Yang, M.; Zeng, Y.; Huang, Z.; Qi, J. Q.; Shi, Q.; Lu, T. Synthesis, Characterization and Sintering of Li_2TiO_3 Nanoparticles Via Low Temperature Solid-State Reaction. *Ceram. Int.* **2020**, *46*, 1816−1823.
(10) Tan, G.; Hu, X.; Wang, S.; Yang, X.; Li, Y.; Yang, Z.; Zhang, Y. A Process for Fabrication of Li_2TiO_3 Ceramic Pebbles with High Mechanical Properties Via Non-Hydrolytic Sol-Gel Method. *Ceram. Int.* **2020**, *46*, 27686−27694.
(11) Guo, H.; Wang, H.; Chen, R.; Gong, Y.; Yang, M.; Ye, D.; Shi, Y.; Shi, Q.; Lu, T. Characterization of Li-Rich Li_2TiO_3 Ceramic Pebbles Prepared by Rolling Method Sintered in Air and Vacuum. *J. Nucl. Mater.* **2021**, *546*, 152786.
(12) Wang, J.; Xu, Y.; Liu, H.; Xiang, M.; Zhou, H.; Zhang, Y.; Luo, G. N.; Qi, Q. Influence of ion irradiations on the microstructure in the tritium breeder material Li_2TiO_3. *Nuclear Inst. and Methods in Physics Research B* **2019**, *450*, 189−194.
(13) Kobayashi, M.; Oya, Y.; Munakata, K.; Okuno, K. Developing a Tritium Release Model for Li_2TiO_3 with Irradiation-Induced Defects. *J. Nucl. Mater.* **2015**, *458*, 22−28.
(14) Liu, W.; Di, J.; Zhang, W.; Xue, L. H.; Yan, Y. W. Influence of Titanium Sources on the Microstructures and Properties of Li_2TiO_3 Ceramics Prepared by Hydrothermal Method. *Fusion Eng. Des.* **2019**, *138*, 364−371.
(15) Gu, S. X.; Ji, B.; Qi, Q.; Wang, J.; Zhou, H.; Zhang, Y.; Luo, G.-N. The Effects of Irradiation and High Temperature on Chemical States in Li_2TiO_3. *Int. J. Hydrogen Energy* **2019**, *44*, 32151−32157.
(16) Azuma, K.; Dover, C.; Grinter, D. C.; Grau-Crespo, R.; Almora-Barrios, N.; Thornton, G.; Oda, T.; Tanaka, S. Scanning Tunneling Microscopy and Molecular Dynamics Study of the Li_2TiO_3 (001) Surface. *J. Phys. Chem. C* **2013**, *117*, 5126−5131.
(17) Azuma, K.; Oda, T.; Tanaka, S. First-Principles Calculations for the Surface Termination of Li_2TiO_3 (001) Surfaces. *J. Nucl. Mater.* **2013**, *442*, S705−S709.
(18) Jiang, Y.; Shi, Y.; Xiang, X.; Qi, J.; Han, Y.; Liao, Z.; Lu, T. Thermodynamic Stabilities of Perfect and Vacancy-Defected Li_2TiO_3 (001) Surfaces from First-Principles Analyses. *Phys. Rev. Appl.* **2019**, *11*, No. 054088.
(19) Fang, Y.; Kong, X.; Yu, Y.; Chen, X.; Gao, T.; Xiao, C.; Lu, T. First-Principles Study of the Effect of Nonmetallic Si Doping on Tritium Release from Li_2TiO_3 (001) Surface. *J. Phys. Chem. C* **2019**, *123*, 6477−6486.
(20) Kuganathan, N.; Kordatos, A.; Fitzpatrick, M. E.; Vovk, R. V.; Chroneos, A. Defect Process and Lithium Diffusion in Li_2TiO_3. *Solid State Ionics* **2018**, *327*, 93−98.
(21) Islam, M. M.; Bredow, T. Lithium Diffusion Pathways in β-Li_2TiO_3: A Theoretical Study. *J. Phys. Chem. C* **2016**, *120*, 7061−7066.
(22) Goswami, K. N.; Murphy, S. T. Influence of Lithium Vacancy Defects on Tritium Diffusion inβ-Li_2TiO_3. *J. Phys. Chem. C* **2020**, *124*, 12286−12294.
(23) Li, K.; Yang, W.; Wang, W. H.; Li, Y. T. First Principles Study of Tritium Diffusion in Li_2TiO_3 Crystal with Lithium Vacancy. *Materials.* **2018**, *11*, 2383.
(24) Kresse, G.; Hafner, J. Ab initio molecular dynamics for liquid metals. *Phys. Rev. B* **1993**, *47*, 558−561.
(25) Kresse, G.; Furthmüller, J. Efficient iterative schemes for ab initio total-energy calculations using a plane-wave basis set. *Phys. Rev. B* **1996**, *54*, 11169−11186.
(26) Huang, G. Y.; Wang, C. Y.; Wang, J. T. Detailed check of the LDA+U and GGA+U corrected method for defect calculations in wurtzite ZnO. *Comput. Phys. Commun.* **2012**, *183*, 1749−1752.
(27) Perdew, J. P.; Burke, K.; Ernzerhof, M. Generalized Gradient Approximation Made Simple. *Phys. Rev. Lett.* **1996**, *77*, 3865−3868.
(28) Blöchl, P. E. Projector augmented-wave method. *Phys. Rev. B* **1994**, *50*, 17953−17979.
(29) Kataoka, K.; Takahashi, Y.; Kijima, N.; Nagai, H.; Akimoto, J.; Idemoto, Y.; Ohshima, K. I. Crystal Growth and Structure Refinement of Monoclinic Li_2TiO_3. *Mater. Res. Bull.* **2009**, *44*, 168−172.

https://doi.org/10.1021/acsomega.2c01532
ACS Omega 2022, 7, 27149−27156